F. Sauerwine
Senior Research Scientist,
Metals and Minerals Research,
Gulf & Western Natural Resources Group,
Palmerton, Pa.

B. Avitzur
Professor of Metallurgy and Materials Science and
Director of Institute for Metal Forming,
Lehigh University, Bethlehem, Pa.
Mem. ASME

Limit Analysis of Hollow Disk Forging

Part 2: Lower Bound

A lower bound for hollow disk forging is presented. The hollow disk is separated into several regions by permissible surfaces of stress discontinuity. The friction stress in each zone is assumed to be either variable or constant; the overall friction stress distribution has characteristics similar to experimentally determined distributions. A statically admissible stress field describes the stress distribution within each deforming zone. The dependence of the relative average pressure, the friction stress distribution and the neutral radius upon friction and ring geometry is given. It is found that only for thin rings is the friction stress constant over most of the interface. Finally, it is proposed that friction factors being measured by use of the mathematically calibrated ring compression test may be somewhat high.

Introduction

A lower bound solution for hollow disk forging [1][1] is presented in this paper. The analytical procedure utilized is very similar to that established by Avitzur [2, 3] for solid disks. The constant shear factor m description of friction and the Mises material assumptions are made.

Derivation

As presented by Prager and Hodge [4], the lower bound theorem states that "among all statically admissible stress fields, the actual one maximizes"

$$\int_{s_v} T_i v_i ds. \tag{1}$$

In the above expression for power, T_i is the normal stress at the tool-workpiece interface (computed from the assumed statically admissible stress field), v_i is the tool velocity, and s represents the area of the tool-workpiece interface.

To be statically admissible, a stress field must meet the imposed boundary conditions, including the assumed friction stress distribution, satisfy the equilibrium equations and obey the Mises' yield criterion. In addition, the relaxed stress continuity requirements, as described in reference [4], must be maintained.

To obtain a lower bound solution, the hollow disk is first divided into six zones as shown in Fig. 1. Within each zone, the stress distribution is to be described by a statically admissible stress field. The radial positions of the cylindrical surfaces of permissible stress discontinuity (R_1, R_2, R_n, R_3, R_4) will be found through maximization of the total power within the constraints imposed by the Mises' yield criterion.

The following boundary conditions are imposed on the stress fields. Since the free surfaces at R_o and R_i cannot support shear stresses,

$$\sigma_{RY}{}^{\mathrm{I}}|_{R_o} = 0 \qquad \text{and} \qquad \sigma_{RY}{}^{\mathrm{VI}}|_{R_i} = 0. \tag{2}$$

If external (p_o) and internal (p_i) pressures restrain these surfaces,

$$\sigma_{RR}{}^{\mathrm{I}}|_{R_o} = -p_o \qquad \text{and} \qquad \sigma_{RR}{}^{\mathrm{VI}}|_{R_i} = -p_i. \tag{3}$$

Additional boundary conditions will be considered after the assumed friction stress τ distribution is described.

The assumed variation of the friction stress τ is illustrated in Fig. 1. τ is assumed to be equal to $-m\sigma_0/\sqrt{3}$ between R_2 and R_1 and $+ m\sigma_0/\sqrt{3}$ from R_4 to R_3. Since τ acts in opposite directions on opposite sides of R_n, stress continuity requires τ to pass through zero at R_n. The friction stress is equivalent to the shear stress at the hollow disk-platen interface ($\tau \equiv \sigma_{RY}|_{Y=T/2}$). Since σ_{RY} is zero along R_o and

[1] Numbers in brackets designate References at end of paper.

Contributed by the Production Engineering Division and presented at the Winter Annual Meeting, Atlanta, Ga., November 27–December 2, 1977, of THE AMERICAN SOCIETY OF MECHANICAL ENGINEERS. Manuscript received at ASME Headquarters June 24, 1977. Paper No. 77-WA/PROD-3.

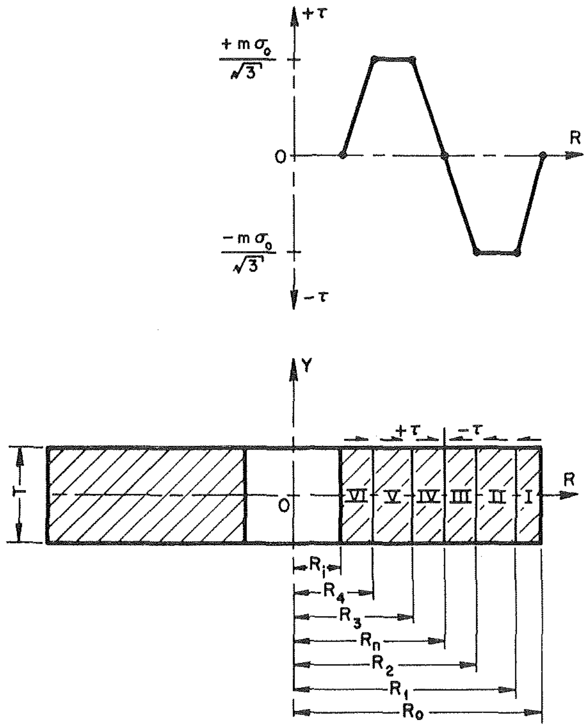

Fig. 1 Assumed friction stress (τ) distribution in hollow disk forging ($R_n > R_i$)

R_i (equations (2)), τ must also be zero at these radial positions. All increases and decreases in τ are assumed to be linear. This distribution has characteristics similar to the friction stress distributions determined experimentally by Unksov [5; Figs. 51, 52, and 61] for bar forging under plane strain conditions.

The remaining boundary conditions result from friction at the ring-platen interface.

$$\sigma_{RY}{}^{\mathrm{I}}|_{Y=T/2} = -\frac{m\sigma_o}{\sqrt{3}}\left(\frac{R_o - R}{R_o - R_1}\right) \tag{4}$$

$$\sigma_{RY}{}^{\mathrm{II}}|_{Y=T/2} = -\frac{m\sigma_o}{\sqrt{3}} \tag{5}$$

$$\sigma_{RY}{}^{\mathrm{III}}|_{Y=T/2} = -\frac{m\sigma_o}{\sqrt{3}}\left(\frac{R - R_n}{R_2 - R_n}\right) \tag{6}$$

$$\sigma_{RY}{}^{\mathrm{IV}}|_{Y=T/2} = \frac{m\sigma_o}{\sqrt{3}}\left(\frac{R_n - R}{R_n - R_3}\right) \tag{7}$$

$$\sigma_{RY}{}^{\mathrm{V}}|_{Y=T/2} = \frac{m\sigma_o}{\sqrt{3}} \tag{8}$$

$$\sigma_{RY}{}^{\mathrm{VI}}|_{Y=T/2} = \frac{m\sigma_o}{\sqrt{3}}\left(\frac{R - R_i}{R_4 - R_i}\right) \tag{9}$$

The shear stress acts in opposite directions on opposite sides of $R = R_n$ and $Y = 0$. Therefore, σ_{RY} must pass through zero at these positions.

$$\sigma_{RY}{}^{\mathrm{III}}|_{R_n} = \sigma_{RY}{}^{\mathrm{IV}}|_{R_n} = 0 \tag{10}$$

$$\sigma_{RY}{}^{\mathrm{I-VI}}|_{Y=0} = 0 \tag{11}$$

Since a hollow disk is axisymmetric, the stress components are independent of Θ and the shear stresses $\sigma_{R\Theta}$ and $\sigma_{\Theta Y}$ vanish. The equilibrium equations given by equations (7.2) of reference [3] reduce to

$$\left.\begin{aligned} &\frac{\partial\sigma_{RR}}{\partial R} + \frac{\partial\sigma_{RY}}{\partial Y} + \frac{\sigma_{RR} - \sigma_{\Theta\Theta}}{R} = 0 \\ &\frac{\partial\sigma_{RY}}{\partial R} + \frac{\partial\sigma_{YY}}{\partial Y} + \frac{\sigma_{RY}}{R} = 0. \end{aligned}\right\} \tag{12}$$

If the restriction that $\sigma_{RR} = \sigma_{\Theta\Theta}$ (When $\dot{\epsilon}_{RR} = \dot{\epsilon}_{\Theta\Theta}$ as assumed in solid disks [2, 3], it follows from the Mises stress-strain rate law

$$\dot{\epsilon}_{ij} = \mu S_{ij} \tag{13}$$

and

$$S_{ij} = \sigma_{ij} - S\delta_{ij} \tag{14}$$

that the corresponding stress components are equal.) is imposed on the stress field, the equilibrium equations become

$$\left.\begin{aligned} &\frac{\partial\sigma_{RR}}{\partial R} + \frac{\partial\sigma_{RY}}{\partial Y} = 0 \\ &\frac{\partial\sigma_{RY}}{\partial R} + \frac{\partial\sigma_{YY}}{\partial Y} + \frac{\sigma_{RY}}{R} = 0. \end{aligned}\right\} \tag{15}$$

With this restriction, the stress field deviates still farther from the exact field, and the resulting solution becomes lower. However, if this sacrifice in accuracy is made, the calculations are simplified.

For an axisymmetric state of stress, the Mises yield criterion is written as

$$\frac{1}{6}\left[(\sigma_{RR} - \sigma_{\Theta\Theta})^2 + (\sigma_{\Theta\Theta} - \sigma_{YY})^2 + (\sigma_{YY} - \sigma_{RR})^2\right] + \sigma_{YR}{}^2 \leqq \frac{\sigma_o{}^2}{3}. \tag{16}$$

Substituting $\sigma_{RR} = \sigma_{\Theta\Theta}$ into inequality (16) and then rearranging to obtain a convenient form of the criterion gives

$$|\sigma_{RR} - \sigma_{YY}| \leq \sigma_o\sqrt{1 - 3\left(\frac{\sigma_{RY}}{\sigma_o}\right)^2}. \tag{17}$$

To maintain equilibrium, the radial σ_{RR} and shear σ_{RY} stresses must be continuous across the cylindrical surfaces at R_1, R_2, R_n, R_3 and R_4. For instance, at R_1,

$$\sigma_{RR}{}^{\mathrm{I}}|_{R_1} = \sigma_{RR}{}^{\mathrm{II}}|_{R_1}; \quad \sigma_{RY}{}^{\mathrm{I}}|_{R_1} = \sigma_{RY}\mathrm{II}|_{R_1}. \tag{18}$$

However, the axial stress is permitted to be discontinuous [4]

$$\sigma_{YY}{}^{\mathrm{I}}|_{R_1} \neq \sigma_{YY}{}^{\mathrm{II}}|_{R_1}; \quad \sigma_{YY}{}^{\mathrm{II}}|_{R_2} \neq \sigma_{YY}{}^{\mathrm{III}}|_{R_2}\ \text{etc.} \tag{19}$$

Nomenclature

m = Constant shear factor
m_c = Critical constant shear factor
p_{ave} = Average pressure
p_i = Internal pressure
p_o = External pressure
R, Θ, Y = Axes of a cylindrical coordinate system
R_i = Internal radius
R_n = Neutral radius
R_o = Outer radius
R_1, R_2, R_n, R_3, R_4 = Radial positions of cylindrical surfaces of permissible stress discontinuity
S = Hydrostatic stress
S_{ij} = Stress deviator component
s = Surface
T = Thickness
T_i = Normal stress at tool-material interface
$\dot{U}$ = Platen velocity
v_i = Velocity
δ_{ij} = Kronecker delta: a unit tensor where, if $i = j$, then $\delta_{ij} = 1$ and if $i \neq j$, then $\delta_{ij} = 0$
$\dot{\epsilon}_{ij}$ = Strain rate component
μ = Scalar function of strain rates
σ_{ij} = Stress component
σ_o = Yield limit in uniaxial tensile test
τ = Friction stress
I, II, III, . . . Zone numbers

at these boundaries since this relaxation does not upset the equilibrium. An example of a surface of stress discontinuity is the interface between two cylinders which have been shrink-fitted together. In this case, the circumferential stress is discontinuous.

To initiate the determination of a statically admissible stress field in zone I, the distribution of the shear stress $\sigma_{RY}{}^{\mathrm{I}}$ is assumed. The following distribution, which is assumed to be linear in R and Y, obeys the boundary conditions in equations (2), (4) and (11).

$$\sigma_{RY}{}^{\mathrm{I}} = -m \frac{\sigma_o}{\sqrt{3}} \left(\frac{Y}{T/2}\right) \left(\frac{R_o - R}{R_o - R_1}\right) \tag{20}$$

The derivative of $\sigma_{RY}{}^{\mathrm{I}}$ with respect to Y is

$$\frac{\partial \sigma_{RY}{}^{\mathrm{I}}}{\partial Y} = -m \frac{\sigma_o}{\sqrt{3}} \left(\frac{1}{T/2}\right) \left(\frac{R_o - R}{R_o - R_1}\right). \tag{21}$$

Substitution of equation (21) into the first of equations (15) and then integration yields $\sigma_{RR}{}^{\mathrm{I}}$.

$$\sigma_{RR}{}^{\mathrm{I}} = + \frac{\sigma_o}{\sqrt{3}} \left(\frac{m}{T/2}\right) \left(\frac{1}{R_o - R_1}\right) \left(R_o R - \frac{R^2}{2}\right) + f^{\mathrm{I}}(Y) \tag{22}$$

The integration constant $[f^I(Y)]$ is found by meeting the boundary condition at R_o (equation (3)).

$$f^{\mathrm{I}}(Y) = - \frac{\sigma_o}{\sqrt{3}} \left(\frac{m}{T/2}\right) \left(\frac{1}{R_o - R_1}\right) \left(\frac{R_o{}^2}{2}\right) - p_0 \tag{23}$$

and

$$\sigma_{RR}{}^{\mathrm{I}} = - \frac{\sigma_0}{\sqrt{3}} \left[\left(\frac{m}{2}\right) \left(\frac{1}{T/2}\right) \frac{(R_o - R)^2}{R_o - R_1} + \left(\frac{p_o}{\sigma_o/\sqrt{3}}\right) \right] \tag{24}$$

Taking the derivative of $\sigma_{RY}{}^{\mathrm{I}}$ (equation (20)) with respect to R,

$$\frac{\partial \sigma_{RY}{}^{\mathrm{I}}}{\partial R} = + m \frac{\sigma_o}{\sqrt{3}} \left(\frac{Y}{T/2}\right) \left(\frac{1}{R_o - R_1}\right) \tag{25}$$

substituting equations (20) and (25) into the second of equations (15) and then integrating leads to

$$\sigma_{YY}{}^{\mathrm{I}} = - m \frac{\sigma_o}{\sqrt{3}} \left(\frac{1}{T/2}\right) \left(\frac{2 - R_o/R}{R_o - R_1}\right) \left(\frac{Y^2}{2}\right) + f^{\mathrm{I}}(R). \tag{26}$$

Since no boundary conditions are imposed on the axial stress σ_{YY}, the expression for $f^{\mathrm{I}}(R)$ is determined from the Mises yield criterion. Substituting equations (24), (26) and (20) into inequality (17) gives

$$\left| - \frac{\sigma_o}{\sqrt{3}} \frac{m}{T} \frac{1}{R_o - R_1} \left[(R_o - R)^2 - \left(2 - \frac{R_o}{R}\right) Y^2 \right] - p_o - f^{\mathrm{I}}(R) \right| \leq \sigma_o \times \sqrt{1 - m^2 \left(\frac{Y}{T/2}\right)^2 \left(\frac{R_o - R}{R_o - R_1}\right)^2}, \tag{27}$$

which leads to

$$\left.\begin{aligned} & -f_1{}^{\mathrm{I}}(R, Y) \leqslant -f_2{}^{\mathrm{I}}(R, Y) - f^{\mathrm{I}}(R) \leqslant f_1{}^{\mathrm{I}}(R, Y) \\ & \text{or} \\ & f_1{}^{\mathrm{I}}(R, Y) - f_2{}^{\mathrm{I}}(R, Y) \geqslant f^{\mathrm{I}}(R) \geqslant -f_1{}^{\mathrm{I}}(R, Y) - f_2{}^{\mathrm{I}}(R, Y), \\ & \text{where} \\ & f_1{}^{\mathrm{I}}(R, Y) = + \sigma_o \sqrt{1 - m^2 \left(\frac{Y}{T/2}\right)^2 \left(\frac{R_o - R}{R_o - R_1}\right)^2} \\ & \text{and} \\ & f_2{}^{\mathrm{I}}(R, Y) = + \frac{\sigma_o}{\sqrt{3}} \frac{m}{T} \frac{1}{R_o - R_1} \left[(R_o - R)^2 - \left(2 - \frac{R_o}{R}\right) Y^2 \right] + p_o. \end{aligned}\right\} \tag{28}$$

Setting $f^{\mathrm{I}}(R)$ equal to the right side rather than the left side of the above inequality results in a larger negative value for σ_{YY} and subsequently an upper, lower bound. However, $f^{\mathrm{I}}(R)$ must only be a function of R if the equilibrium equations are to be obeyed. Letting $Y = T/2$ (explained in paragraph following equations (36)) and hence satisfying inequality (28) only at $Y = T/2$, $f^{\mathrm{I}}(R)$ becomes

$$f^{\mathrm{I}}(R) = - \sigma_o \sqrt{1 - m^2 \left(\frac{R_o - R}{R_o - R_1}\right)^2} - \frac{\sigma_o}{\sqrt{3}} \frac{m}{T} \frac{1}{R_o - R_1} \times \left[(R_o - R)^2 - \left(2 - \frac{R_o}{R}\right) \frac{T^2}{4} \right] - p_o, \tag{29}$$

and $\sigma_{YY}{}^{\mathrm{I}}$ is

$$\sigma_{YY}{}^{\mathrm{I}} = -\sigma_o \sqrt{1 - m^2 \left(\frac{R_o - R}{R_o - R_1}\right)^2} - p_o - \frac{\sigma_o}{\sqrt{3}} \frac{m}{T} \frac{1}{R_o - R_1} \times \left[\left(2 - \frac{R_o}{R}\right) \left(Y^2 - \frac{T^2}{4}\right) + (R_o - R)^2 \right]. \tag{30}$$

The derived stress field must satisfy the Mises yield criterion throughout zone I. The assumption is made that if the yield criterion is obeyed at the corners of each zone, it is obeyed throughout the zone. Substituting equations (24), (30) and (20) into inequality (17) gives

$$\left| + \sigma_o \sqrt{1 - m^2 \left(\frac{R_o - R}{R_o - R_1}\right)^2} + \frac{\sigma_o}{\sqrt{3}} \frac{m}{T} \left[\frac{\left(2 - \frac{R_o}{R}\right) \left(Y^2 - \frac{T^2}{4}\right)}{R_o - R_1} \right] \right| \leq \sigma_o \sqrt{1 - m^2 \left(\frac{Y}{T/2}\right)^2 \left(\frac{R_o - R}{R_o - R_1}\right)^2}. \tag{31}$$

At $Y = T/2$, the inequality is satisfied for all R values. At $Y = 0$,

$$\left| \sigma_o \sqrt{1 - m^2 \left(\frac{R_o - R}{R_o - R_1}\right)^2} - \frac{\sigma_o}{\sqrt{3}} \frac{m}{T} \frac{\left(2 - \frac{R_o}{R}\right) \frac{T^2}{4}}{R_o - R_1} \right| \leq \sigma_o. \tag{32}$$

Evaluating inequality (32) at $R = R_o$ and solving for R_1/R_o yields

$$\frac{R_1}{R_o} \leq 1 - \frac{1}{8\sqrt{3}} \frac{m}{R_o/T}. \tag{33}$$

The following additional restrictions are obtained after substituting $R = R_1$ into inequality (32).

$$\left.\begin{aligned} & \frac{1}{2} - A \left(1 + \frac{1}{2} \sqrt{\left(\frac{1}{A}\right)^2 + 4}\right) \leq \frac{R_1}{R_o} \leq \frac{1}{2} - A \left(1 - \frac{1}{2} \sqrt{\left(\frac{1}{A}\right)^2 + 4}\right), \\ & \text{where} \\ & A = \frac{m}{4\sqrt{3}(1 + \sqrt{1 - m^2}) R_o/T}. \end{aligned}\right\} \tag{34}$$

$$\left.\begin{aligned} & \frac{1}{2} - B \left(1 - \frac{1}{2} \sqrt{\left(\frac{1}{B}\right)^2 + 4}\right) \leq \frac{R_1}{R_o} \leq \frac{1}{2} - B \left(1 + \frac{1}{2} \sqrt{\left(\frac{1}{B}\right)^2 + 4}\right), \\ & \text{where} \\ & B = \frac{m}{4\sqrt{3}(\sqrt{1 - m^2} - 1) R_o/T}. \end{aligned}\right\} \tag{35}$$

Thus, the following stress field for zone I is statically admissible if the permissible surface of stress discontinuity at R_1 remains within the limits (inequalities (33), (34) and (35)) governed by the yield criterion.

$$\left.\begin{aligned} & \frac{\sigma_{RY}{}^{\mathrm{I}}}{\sigma_o} = - \frac{2}{\sqrt{3}} m \frac{R_o}{T} \left(\frac{Y}{R_o}\right) \left(\frac{1 - \frac{R}{R_o}}{1 - \frac{R_1}{R_o}}\right); \quad \frac{\sigma_{R\theta}{}^{\mathrm{I}}}{\sigma_o} = \frac{\sigma_{\theta Y}{}^{\mathrm{I}}}{\sigma_o} = 0 \\ & \frac{\sigma_{RR}{}^{\mathrm{I}}}{\sigma_o} = \frac{\sigma_{\theta\theta}{}^{\mathrm{I}}}{\sigma_o} = - \frac{1}{\sqrt{3}} \frac{m R_o}{T} \left[\frac{\left(1 - \frac{R}{R_o}\right)^2}{1 - \frac{R_1}{R_o}} \right] - \frac{p_o}{\sigma_o} \end{aligned}\right\} \tag{36}$$

$$\frac{\sigma_{YY}{}^{\mathrm{I}}}{\sigma_o} = -\sqrt{1 - m^2\left(\frac{1-\frac{R}{R_o}}{1-\frac{R_1}{R_o}}\right)^2} - \frac{1}{\sqrt{3}}\frac{mR_o}{T} \times \left\langle \frac{\left(1-\frac{R}{R_o}\right)^2 + \left(\frac{2\frac{R}{R_o}-1}{R/R_o}\right)\left[\left(\frac{Y}{R_o}\right)^2 - \frac{1}{4}\frac{1}{(R_o/T)^2}\right]}{1-\frac{R_1}{R_o}} \right\rangle - \frac{p_o}{\sigma_o}$$

At this point, the reason can be given for choosing $Y = T/2$ rather than $Y = 0$ when determining an expression for $f^{\mathrm{I}}(R)$. Letting $Y = 0$ results in a stress field with restrictions on R_1/R_o which cannot be met. To be specific, at the position $Y = T/2$ and $R = R_o$,

$$\frac{1}{4\sqrt{3}} m \frac{T}{R_o - R_1} \leq 0. \tag{37}$$

Obviously, R_1 cannot be greater than R_o.

As in zone I, the first step in the determination of a statically admissible stress field for zone II is to assume a distribution of $\sigma_{RY}{}^{\mathrm{II}}$. In addition to meeting the boundary conditions in equations (5) and (11), $\sigma_{RY}{}^{\mathrm{II}}$ must maintain stress continuity across the surface at R_1.

$$\sigma_{RY}{}^{\mathrm{II}}|_{R_1} = \sigma_{RY}{}^{\mathrm{I}}|_{R_1} = -\frac{m\sigma_o}{\sqrt{3}}\frac{Y}{T/2} \tag{38}$$

The assumed distribution of $\sigma_{RY}{}^{\mathrm{II}}$ is

$$\sigma_{RY}{}^{\mathrm{II}} = -\frac{m\sigma_o}{\sqrt{3}}\frac{Y}{T/2}. \tag{39}$$

The derivatives of the shear stress $\sigma_{RY}{}^{\mathrm{II}}$ are

$$\frac{\partial \sigma_{RY}{}^{\mathrm{II}}}{\partial Y} = -\frac{m\sigma_o}{\sqrt{3}}\frac{1}{T/2} \quad \text{and} \quad \frac{\partial \sigma_{RY}{}^{\mathrm{II}}}{\partial R} = 0. \tag{40}$$

Substituting the first of equations (40) into the first of equations (15) and then integrating leads to

$$\sigma_{RR}{}^{\mathrm{II}} = \frac{m\sigma_o}{\sqrt{3}}\left(\frac{1}{T/2}\right)R + f^{\mathrm{II}}(Y). \tag{41}$$

The function $f^{\mathrm{II}}(Y)$ enables $\sigma_{RR}{}^{\mathrm{II}}$ to meet the stress continuity requirement at R_1.

$$\sigma_{RR}{}^{\mathrm{II}}|_{R_1} = \sigma_{RR}{}^{\mathrm{I}}|_{R_1} = -\frac{\sigma_o}{\sqrt{3}}\left[\frac{m}{T}(R_o - R_1) + \frac{p_o}{\sigma_o/\sqrt{3}}\right] \tag{42}$$

$\sigma_{RR}{}^{\mathrm{II}}$ becomes

$$\sigma_{RR}{}^{\mathrm{II}} = -\frac{\sigma_o}{\sqrt{3}}\left[\left(\frac{m}{T}\right)(R_o + R_1 - 2R) + \frac{p_o}{\sigma_o/\sqrt{3}}\right]. \tag{43}$$

The axial stress $\sigma_{YY}{}^{\mathrm{II}}$ and the yield criterion restrictions are found according to the procedure used in zone I. The stress field in zone II

$$\left.\begin{aligned}
&\frac{\sigma_{RY}{}^{\mathrm{II}}}{\sigma_o} = -\frac{2}{\sqrt{3}}\frac{mR_o}{T}\left(\frac{Y}{R_o}\right); \frac{\sigma_{R\Theta}{}^{\mathrm{II}}}{\sigma_o} = \frac{\sigma_{\Theta Y}{}^{\mathrm{II}}}{\sigma_o} = 0\\
&\frac{\sigma_{RR}{}^{\mathrm{II}}}{\sigma_o} = \frac{\sigma_{\Theta\Theta}{}^{\mathrm{II}}}{\sigma_o} = -\frac{1}{\sqrt{3}}\frac{mR_o}{T}\left(1 + \frac{R_1}{R_o} - 2\frac{R}{R_o}\right) - \frac{p_o}{\sigma_o}\\
&\frac{\sigma_{YY}{}^{\mathrm{II}}}{\sigma_o} = -\sqrt{1-m^2} - \frac{1}{\sqrt{3}}\frac{mR_o}{T}\left[\left(1 + \frac{R_1}{R_o} - 2\frac{R}{R_o}\right)\right.\\
&\quad \left. + \frac{1}{4}\frac{1}{(R_o/T)^2}\frac{1}{R/R_o} - \left(\frac{Y}{R_o}\right)^2\frac{1}{R/R_o}\right] - \frac{p_o}{\sigma_o}
\end{aligned}\right\} \tag{44}$$

is statically admissible if

$$\frac{R_2}{R_o} \geq \frac{m}{4\sqrt{3}\,(1 - \sqrt{1-m^2})R_o/T}. \tag{45}$$

Statically admissible stress fields for zones III, IV, and V are determined in a manner similar to that used for zones I and II. The only difference is that in zones III and IV, the expressions for $f^{\mathrm{III}}(R)$ and $f^{\mathrm{IV}}(R)$ satisfy the yield criterion at $Y = 0$ instead of $Y = T/2$. The results are found in the Appendix.

The procedure for zones I–V must be altered for zone VI. The radial stress in zone VI must not only meet the continuity requirement at R_4 but also the boundary condition at R_i (equation (3)). If $\sigma_{RR}{}^{\mathrm{VI}}$ were derived from the first of equations (15) after assuming $\sigma_{RY}{}^{\mathrm{VI}}$, only one of these conditions could be met. This difficulty can be avoided by first assuming linear distributions for both $\sigma_{RY}{}^{\mathrm{VI}}$ and $\sigma_{RR}{}^{\mathrm{VI}}$ which meet all conditions and then lifting the restriction that $\sigma_{RR}{}^{\mathrm{VI}}$ is equal to $\sigma_{\Theta\Theta}{}^{\mathrm{VI}}$. Therefore, to be statically admissible, the stress field in zone VI must obey the equilibrium equations in equations (12) and the Mises yield criterion in inequality (16). The statically admissible stress field for zone VI is given in the Appendix.

The lower bound on the relative average forging pressure $p_{\mathrm{ave}}/\sigma_o$ is computed from the axial stress components at the hollow disk-platen interface. The total lower bound on power is found by applying expression (46) to each of zones I–VI and then summing these terms.

$$\int_{s_v} T_i v_i ds = \int (-\sigma_{YY}|_{Y=T/2})(\dot{U})(2\pi R dR)$$
$$= -2\pi\dot{U}\sigma_o R_o{}^2 \int \frac{\sigma_{YY}}{\sigma_o}\Big|_{Y=T/2}\left(\frac{R}{R_o}\right) d\left(\frac{R}{R_o}\right). \tag{46}$$

Equating this total power to the externally supplied power (equation (11), Part 1) results in

$$\left.\begin{aligned}
\frac{p_{\mathrm{ave}}}{\sigma_o} = \frac{1}{1-\left(\frac{R_i}{R_o}\right)^2}\Bigg\{&\left(1 - \frac{R_1}{R_o}\right)\left(\sqrt{1-m^2} + \frac{\sin^{-1} m}{m}\right)\\
&+ \frac{2}{3}\left(1 - \frac{R_1}{R_o}\right)^2 \frac{1}{m^2}\left(\sqrt{(1-m^2)^3} - 1\right)\\
&+ \frac{1}{6\sqrt{3}}\frac{mR_o}{T}\left[1 + \frac{R_1}{R_o} + \left(\frac{R_1}{R_o}\right)^2 + \left(\frac{R_1}{R_o}\right)^3 - \frac{R_2}{R_o}\left(\frac{R_n}{R_o}\right)^2\right.\\
&- \left(\frac{R_2}{R_o}\right)^2\frac{R_n}{R_o} - \left(\frac{R_2}{R_o}\right)^3 - \frac{R_n}{R_o}\left(\frac{R_3}{R_o}\right)^2 - \left(\frac{R_n}{R_o}\right)^2\frac{R_3}{R_o} - 2\left(\frac{R_n}{R_o}\right)^3\\
&\left. - \left(\frac{R_3}{R_o}\right)^3 + \frac{R_4}{R_o}\left(\frac{R_i}{R_o}\right)^2 + \left(\frac{R_4}{R_o}\right)^2\frac{R_i}{R_o} + \left(\frac{R_4}{R_o}\right)^3 + \left(\frac{R_i}{R_o}\right)^3\right]\\
&- \frac{1}{2\sqrt{3}}\frac{m}{R_o/T}\left(\frac{R_2}{R_o} + \frac{R_3}{R_o}\right) + \left[\left(\frac{R_2}{R_o}\right)^2 - \left(\frac{R_3}{R_o}\right)^2\right]\\
&+ \sqrt{1-m^2}\left[\left(\frac{R_1}{R_o}\right)^2 - \left(\frac{R_2}{R_o}\right)^2 + \left(\frac{R_3}{R_o}\right)^2 - \left(\frac{R_4}{R_o}\right)^2\right] + \frac{p_o}{\sigma_o}\\
&- \frac{p_i}{\sigma_o}\left(\frac{R_i}{R_o}\right)^2 + \int_{R_i/R_o}^{R_4/R_o}\sqrt{H\left(\frac{R}{R_0}\right) - K\left(\frac{R}{R_o}\right)}\left(\frac{R}{R_o}\right)d\left(\frac{R}{R_o}\right)\Bigg\}
\end{aligned}\right\} \tag{47}$$

where

$$H\left(\frac{R}{R_o}\right) = 4\left[1 - m^2\left(\frac{\frac{R}{R_o} - \frac{R_i}{R_o}}{\frac{R_4}{R_0} - \frac{R_i}{R_o}}\right)^2\right]$$

$$K\left(\frac{R}{R_o}\right) = 3\left\langle\left\{\frac{1}{\sqrt{3}}\frac{mR_o}{T}\left[\left(1 + \frac{R_1}{R_o} - \frac{R_2}{R_o} - 2\frac{R_n}{R_o}\right.\right.\right.\right.$$
$$\left.\left. - \frac{R_3}{R_o} + 2\frac{R_4}{R_o}\right) - 2\left(\frac{R}{R_o} - \frac{R_i}{R_o}\right)\right]$$

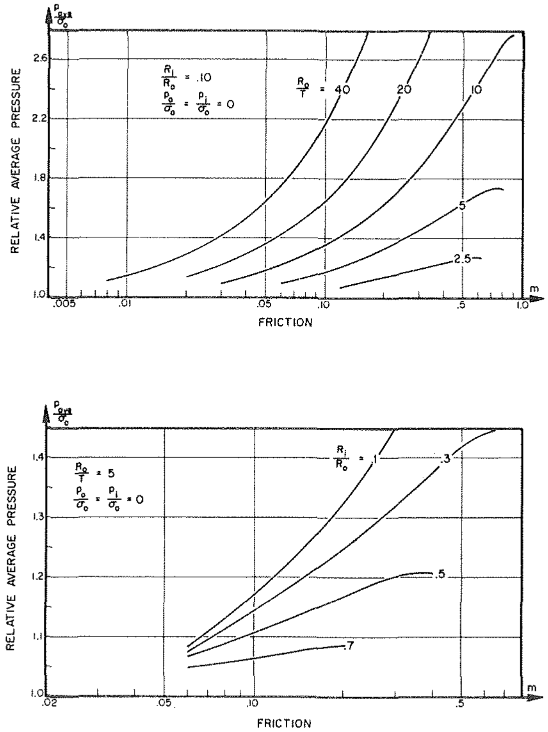

Fig. 2(a),(b) Lower bound on the relative average pressure

$$+\left(\frac{p_o}{\sigma_o}-\frac{p_i}{\sigma_o}\right)\Bigg]\left(\frac{\frac{R}{R_o}}{\frac{R_4}{R_o}-\frac{R_i}{R_o}}\right)\Bigg\rangle^2\Bigg|$$

Integration of the last term in equation (47) is performed numerically.

Within the limits governed by the Mises yield criterion, the values of R_1/R_o, R_2/R_o, R_n/R_o, R_3/R_o and R_4/R_o maximize p_{ave}/σ_o. These radial positions are found through a computer program [1]. In Figs. 2(a) and 2(b), the relative average pressure p_{ave}/σ_o is plotted as a function of m for various R_o/T and R_i/R_o combinations. Corresponding R_n/R_o values are presented in Figs. 3(a) and 3(b). The solution terminates when R_2/R_o becomes equal to R_1/R_o. This eventually occurs as m decreases from m_c, the critical (maximum) value of the constant shear factor (to be discussed).

For the special case of a solid disk ($R_n = R_3 = R_4 = R_i = 0$),$p_{ave/\sigma o}$ in equation (47) reduces to equation 7.77 of reference [3], the lower bound solution for a solid disk.

Discussion

Friction Hill. The presence of a friction stress at the platen-hollow disk interface results in the "friction hill" phenomenon: an increase in the interface pressure from the edges to the neutral radius R_n. The relative shear stress distribution at the hollow disk surface $\sigma_{RY}/\sigma_o|_{Y=T/2}$ (equivalent to the relative friction stress τ/σ_o) predicted by the lower bound through maximization (within yield criterion limits) of p_{ave}/σ_o in equation (47) and the corresponding relative axial stress distribution at the interface $-\sigma_{YY}/\sigma_o|_{Y=T/2}$ (equivalent to relative interface pressure) are plotted in Fig. 4 for m = .4, R_o/T = 10/1 and R_i/R_o = 1/10. Moving outward from R_i and inward from R_1 toward R_n, $-\sigma_{YY}/\sigma_o|_{Y=T/2}$ increases with the allowed discontinuities, reaching a maximum at R_n. A linear increase is observed where τ/σ_o is constant. However, since the friction stress drops to zero at R_n, the peak becomes rounded-off. The "friction hill" is shifted upward with increased m and R_o/T and decreased R_i/R_o.

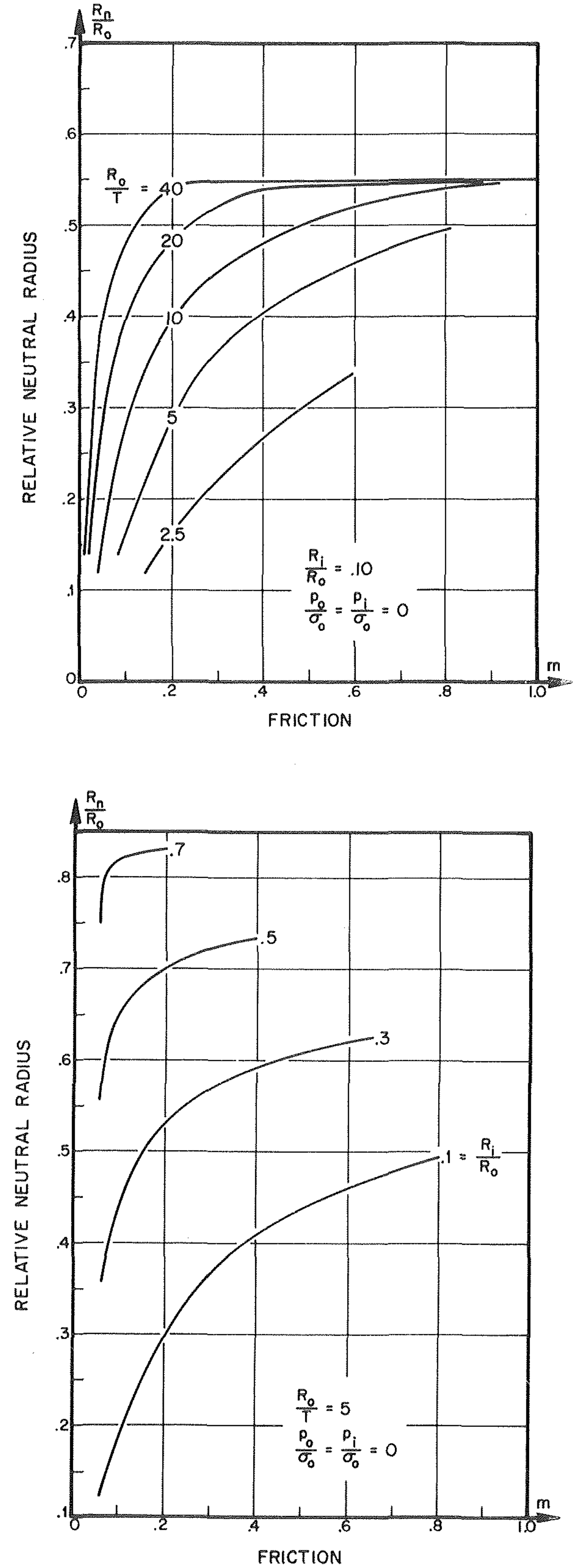

Fig. 3(a),(b) Relative neutral radius predictions of lower bound

Similar friction and axial stress behavior has been determined experimentally by Unksov [5; Figs. 51, 52 and 61] for forging bars under plane strain conditions. Thus it should be noted that the friction and axial stress distributions in Fig. 4 are quite realistic.

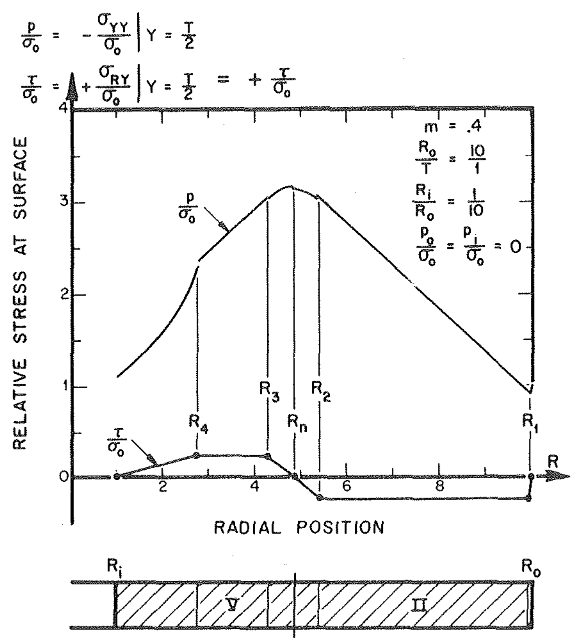

Fig. 4 The relative axial (σ_{YY}/σ_o) and shear (σ_{RY}/σ_o) stress distributions at the hollow disk surface ($Y = T/2$)

Friction Characteristics. The critical value of the constant shear factor m_c maximizes p_{ave}/σ_o. As seen in Figs. 2(*a*) and (*b*), p_{ave}/σ_o increases up to a maximum with increased m. If m becomes greater than m_c, p_{ave}/σ_o drops. Since p_{ave}/σ_o is expected to increase with increased m, the curves are terminated at m_c. The value of m_c increases with increased R_o/T and decreased R_i/R_o.

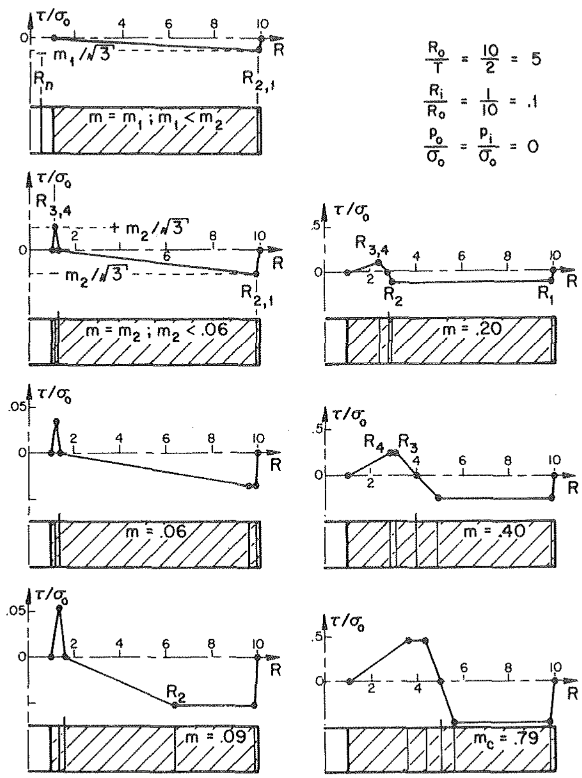

Fig. 5 The effect of the constant shear factor (m) on the relative friction stress (τ/σ_o) distribution

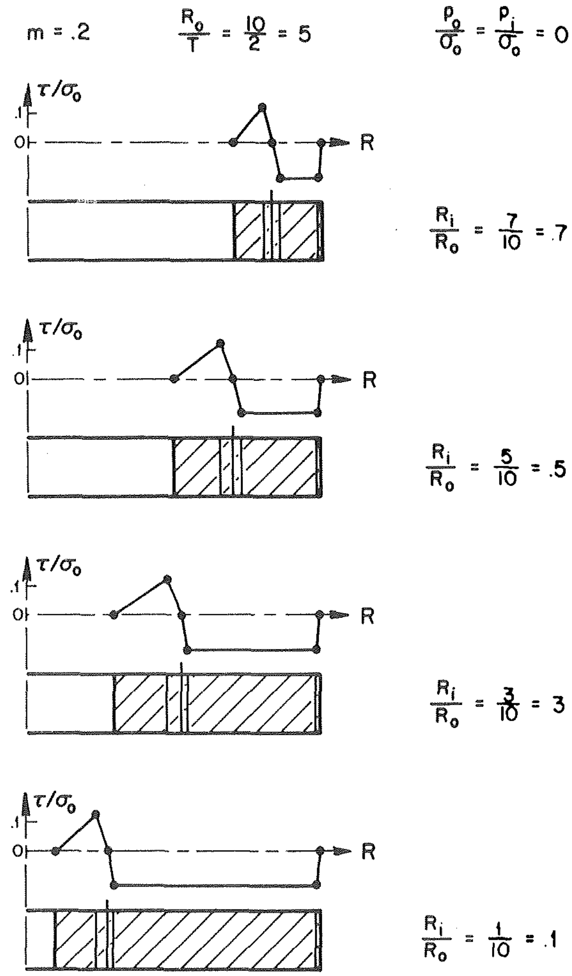

Fig. 6 The effect of the internal radius ratio (R_i/R_o) on the relative friction stress (τ/σ_o) distribution

The critical value of m is always less than one although it becomes quite close to unity for large values of R_o/T. According to the interpretation of this result in "Limit Analysis of Solid Disk and Strip Forging" by Avitzur [2], the shear stress at the hollow disk-platen interface (equivalent to friction stress) never reaches the maximum value of $\sigma_o/\sqrt{3}$; not even for rough, unlubricated surfaces. The maximum shear stresses in the hollow disk occur over surfaces inclined to the interface.

The effect of the constant shear factor m on the relative friction stress τ/σ_o distribution is illustrated in Fig. 5. For a hollow disk with dimensions of $R_o = 10$, $T = 2$, and $R_i = 1$, $m_c = .79$. At this friction level, two zones of constant τ/σ_o exist. For decreased m, R_2, R_n, R_3 and R_4 are located closer to R_i resulting in a wider zone II ($R_1 - R_2$) but a narrower zone $V(R_3 - R_4)$. (See $m = .4$.) Eventually, R_3 becomes equal to R_4 and zone V disappears. (See $m = .2$.) As m is decreased further, the merged R_3 and R_4 and R_n get closer to R_i, and R_2 moves outward (due to restriction in zone II) toward R_1, causing zone II to narrow. (See $m = .09$.) At $m = .06$, R_2 is nearly equal to R_1, and $R_{3,4}$ and R_n are very close to R_i. Since the present computer program [1] must be modified before considering the τ/σ_o distribution for $m = m_2 < .06$ ($R_4 = R_3 = R_{3,4}$; $R_2 = R_1 = R_{2,1}$), the solution is terminated at $m = .06$ as noticed in Figs. 2(a) and (b).

A friction stress distribution is proposed for $m = m_1$ where $0 < m_1 < m_2$. $R_{2,1}$ will be closer to R_o, and R_n will be less than R_i. When $m = 0$, R_n will coincide with the axis of symmetry ($R_n = 0$), and $R_{2,1}$ will be at R_O; the friction stress will be zero.

Fig. 6 illustrates the effect of R_i on the τ/σ_o distribution when $m = .2$, $R_o = 10$ and $T = 2$. As R_i is increased from $R_i = 1$, R_3, R_4, (note

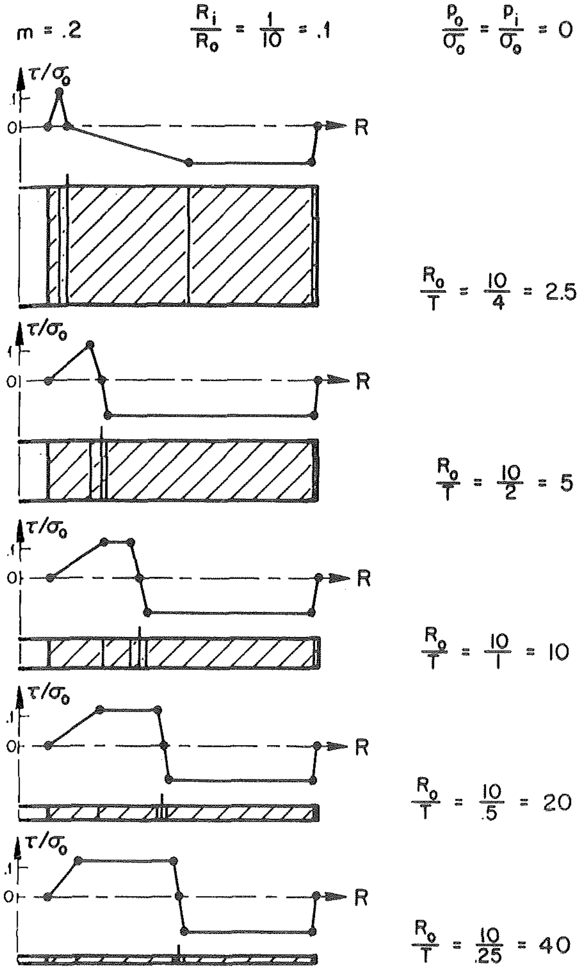

Fig. 7 The effect of the outer radius to thickness ratio (R_o/T) on the relative friction stress (τ/σ_o) distribution

that $R_3 = R_4$), R_n and R_2 move outward, resulting in the reduction in width of zone II.

The τ/σ_o distribution is also a function of the outer radius to thickness ratio R_o/T. Fig. 7 illustrates the dependency for $m = .2$, $R_i = 1$, and $R_o = 10$. At $R_o/T = 10/4$, R_3, $R_4 (R_3 = R_4)$, and R_n are close to R_i while R_2 is much farther from R_i; hence zone II is relatively narrow. For a thinner disk, $R_o/T = 10/2$, R_3, R_4 and R_n are farther outward. Since R_2 is now close to R_n, zone II is quite wide. As T is reduced still further, R_3, R_n, and R_2 move outward with R_3 and R_2 approaching R_n. Since R_4 moves toward R_i, the friction stress becomes constant over most of the interface. The limit of the friction stress distribution as $R_o/T \rightarrow \infty$ is $|\tau| = m\sigma_o/\sqrt{3}$ across the entire interface [1]. This predicted friction stress behavior is in agreement with the experimental results of Unksov [5; Figs. 51, 52, and 61].

Ring Compression Test [6,7]. The parallel velocity field and the neutral radius predictions of the upper bound analysis of Avitzur [3] are utilized to determine a limited segment of a calibration curve for a 6:3:0.5 ring and $m = 0.1$. This curve is represented by a solid line in Fig. 8. If the parallel velocity field [3] and the R_n/R_o values of the lower bound are used to compute a calibration curve for the same conditions, a definite upward shift occurs. Consequently, it is proposed that actual calibration curves are higher than those in references 6 and 7. In other words, the friction factors being measured may be somewhat high.

Conclusions

1. Maximization (within limitations governed by the yield criterion) of the lower bound on power reveals a realistic friction stress

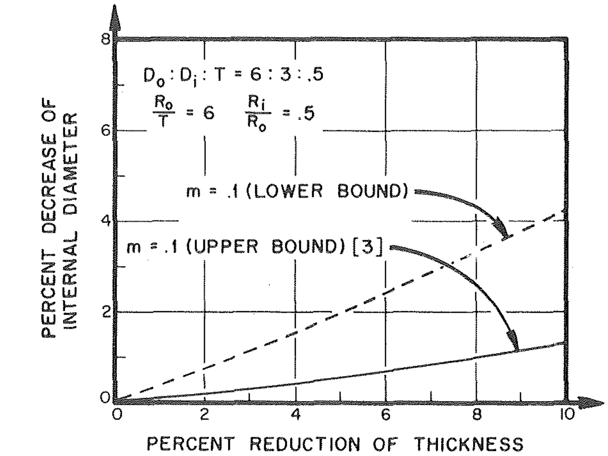

Fig. 8 The effect of using R_n/R_o values predicted by the lower bound to calculate theoretical calibration curve for ring compression test

distribution. The friction stress is predicted to be constant over only a portion of the hollow disk-platen interface or variable across the entire surface, depending upon the friction factor and the ring geometry. Only for a thin ring is the friction stress constant over most of the interface.

2. It is proposed that the friction factors being measured by utilization of the mathematically calibrated ring compression test [6, 7] are somewhat high.

Acknowledgments

Financial support of the National Science Foundation is acknowledged with gratitude. Also, part of this study was financed by internal funds of the Institute for Metal Forming.

References

1 Sauerwine, F. R., "Limit Analysis of Hollow Disk Forging," Ph.D. dissertation, Metallurgy and Materials Science Department, Lehigh University, May, 1971.

2 Avitzur, B., "Limit Analysis of Disk and Strip Forging," International Journal of Machine Tool Design and Research, Vol. 9, 1969, pp. 165–195.

3 Avitzur, B., *Metal Forming: Processes and Analysis*, McGraw-Hill, New York, 1968, Ch. 7.

4 Prager, W., and Hodge, Jr., P. G., *Theory of Perfectly Plastic Solids*, John Wiley and Sons, Inc., New York, 1951.

5 Unksov, E. P., *An Engineering Theory of Plasticity*, Translated by Production Engineering Research Association of Great Britain, Butterworths, London, 1961.

6 Male, A. T. and DePierre, V., "The Validity of Mathematical Solutions for Determining Friction from the Ring Compression Test," *Journal of Lubrication Technology*, TRANS. ASME, July, 1970, pp. 389–397.

7 Abdul, N. A., and Bramley, A. N., "Determination of Yield Stress-Strain Relations Using the Ring Compression Technique," Research Report, Ref. No. SM/8, Department of Mechanical Engineering, University of Leeds, July, 1972.

Appendix

Zone III.

$$\frac{\sigma_{RY}^{\mathrm{III}}}{\sigma_o} = -\frac{2}{\sqrt{3}}\frac{mR_o}{T}\left(\frac{Y}{R_o}\right)\left(\frac{\frac{R}{R_o} - \frac{R_n}{R_o}}{\frac{R_2}{R_o} - \frac{R_n}{R_o}}\right); \frac{\sigma_{R\theta}^{\mathrm{III}}}{\sigma_o} = \frac{\sigma_{\theta Y}^{\mathrm{III}}}{\sigma_o} = 0$$

$$\frac{\sigma_{RR}^{\mathrm{III}}}{\sigma_o} = \frac{\sigma_{\theta\theta}^{\mathrm{III}}}{\sigma_o} = -\frac{1}{\sqrt{3}}\frac{mR_o}{T}\left[\left(1 + \frac{R_1}{R_o} - 2\frac{R_2}{R_o}\right)\right.$$

$$+\left(\frac{\dfrac{R_2}{R_o}-\dfrac{R}{R_o}}{\dfrac{R_2}{R_o}-\dfrac{R_n}{R_o}}\right)\left(\frac{R}{R_o}+\frac{R_2}{R_o}-2\frac{R_n}{R_o}\right)\Bigg]-\frac{p_o}{\sigma_o} \tag{48}$$

$$\frac{\sigma_{YY}{}^{\rm III}}{\sigma_o}=-1-\frac{1}{\sqrt{3}}\frac{mR_o}{T}\Bigg[\left(1+\frac{R_1}{R_o}-2\frac{R_2}{R_o}\right)+\left(\frac{\dfrac{R_2}{R_o}-\dfrac{R}{R_o}}{\dfrac{R_2}{R_o}-\dfrac{R_n}{R_o}}\right)\left(\frac{R}{R_o}+\frac{R_2}{R_o}-2\frac{R_n}{R_o}\right)-\frac{\left(\dfrac{2\dfrac{R}{R_o}-\dfrac{R_n}{R_o}}{R/R_o}\right)\left(\dfrac{Y}{R_o}\right)^2}{R_2/R_o-R_n/R_o}\Bigg]-\frac{p_o}{\sigma_o}$$

$$\frac{R_2}{R_o}\geq\frac{R_n}{R_o}+\frac{1}{8\sqrt{3}}\frac{m}{R_o/T} \tag{49}$$

$$\frac{R_2}{R_o}\leq\frac{1}{2}\frac{R_n}{R_o}+A\left(1-\frac{1}{2}\sqrt{\left(\frac{1}{A}\frac{R_n}{R_o}\right)^2+4}\right)\quad\text{or}$$

$$\frac{R_2}{R_o}\geq\frac{1}{2}\frac{R_n}{R_o}+A\left(1+\frac{1}{2}\sqrt{\left(\frac{1}{A}\frac{R_n}{R_o}\right)^2+4}\right), \tag{50}$$

where A is defined in equation (34).

$$\frac{1}{2}\frac{R_n}{R_o}+C\left(1-\frac{1}{2}\sqrt{\left(\frac{1}{C}\frac{R_n}{R_o}\right)^2+4}\right)\leq\frac{R_2}{R_o}\leq\frac{1}{2}\frac{R_n}{R_o}+C\left(1+\frac{1}{2}\sqrt{\left(\frac{1}{C}\frac{R_n}{R_o}\right)^2+4}\right), \tag{51}$$

where

$$C=\frac{m}{4\sqrt{3}\,(1-\sqrt{1-m^2})R_o/T}.$$

Zone IV.

$$\frac{\sigma_{RY}{}^{\rm IV}}{\sigma_o}=\frac{2}{\sqrt{3}}\frac{mR_o}{T}\left(\frac{Y}{R_o}\right)\left(\frac{\dfrac{R_n}{R_o}-\dfrac{R}{R_o}}{\dfrac{R_n}{R_o}-\dfrac{R_3}{R_o}}\right);\quad\frac{\sigma_{R\Theta}{}^{\rm IV}}{\sigma_o}=\frac{\sigma_{\Theta Y}{}^{\rm IV}}{\sigma_o}=0$$

$$\frac{\sigma_{RR}{}^{\rm IV}}{\sigma_o}=\frac{\sigma_{\Theta\Theta}{}^{\rm IV}}{\sigma_o}=-\frac{1}{\sqrt{3}}\frac{mR_o}{T}\times\left[\left(1+\frac{R_1}{R_o}-\frac{R_2}{R_o}-\frac{R_n}{R_o}\right)-\frac{\left(\dfrac{R_n}{R_o}-\dfrac{R}{R_o}\right)^2}{\left(\dfrac{R_n}{R_o}-\dfrac{R_3}{R_o}\right)}\right]-\frac{p_o}{\sigma_o} \tag{52}$$

$$\frac{\sigma_{YY}{}^{\rm IV}}{\sigma_o}=-1-\frac{1}{\sqrt{3}}\frac{mR_o}{T}\Bigg[\left(1+\frac{R_1}{R_o}-\frac{R_2}{R_o}-\frac{R_n}{R_o}\right)-\frac{\left(\dfrac{R_n}{R_o}-\dfrac{R}{R_o}\right)^2-\left(\dfrac{2\dfrac{R}{R_o}-\dfrac{R_n}{R_o}}{R/R_o}\right)\left(\dfrac{Y}{R_o}\right)^2}{\left(\dfrac{R_n}{R_o}-\dfrac{R_3}{R_o}\right)\left(\dfrac{R_n}{R_o}-\dfrac{R_3}{R_o}\right)}\Bigg]-\frac{p_o}{\sigma_o}$$

$$\frac{R_3}{R_o}\leq\frac{R_n}{R_o}-\frac{1}{8\sqrt{3}}\frac{m}{R_o/T} \tag{53}$$

$$\frac{1}{2}\frac{R_n}{R_o}-A\left(1+\frac{1}{2}\sqrt{\left(\frac{1}{A}\frac{R_n}{R_o}\right)^2+4}\right)\leq\frac{R_3}{R_o}\leq\frac{1}{2}\frac{R_n}{R_o}-A\left(1-\frac{1}{2}\sqrt{\left(\frac{1}{A}\frac{R_n}{R_o}\right)^2+4}\right) \tag{54}$$

$$\frac{R_3}{R_o}\leq\frac{1}{2}\frac{R_n}{R_o}-C\left(1+\frac{1}{2}\sqrt{\left(\frac{1}{C}\frac{R_n}{R_o}\right)^2+4}\right)\quad\text{or}$$

$$\frac{R_3}{R_o}\geq\frac{1}{2}\frac{R_n}{R_o}-C\left(1-\frac{1}{2}\sqrt{\left(\frac{1}{C}\frac{R_n}{R_o}\right)^2+4}\right) \tag{55}$$

Zone V.

$$\frac{\sigma_{RY}{}^{\rm V}}{\sigma_o}=\frac{2}{\sqrt{3}}\frac{mR_o}{T}\left(\frac{Y}{R_o}\right);\quad\frac{\sigma_{R\Theta}{}^{\rm V}}{\sigma_o}=\frac{\sigma_{\Theta Y}{}^{\rm V}}{\sigma_o}=0$$

$$\frac{\sigma_{RR}{}^{\rm V}}{\sigma_o}=\frac{\sigma_{\Theta\Theta}{}^{\rm V}}{\sigma_o}=-\frac{1}{\sqrt{3}}\frac{mR_o}{T}\times\left(1+\frac{R_1}{R_o}-\frac{R_2}{R_o}-2\frac{R_n}{R_o}-\frac{R_3}{R_o}+2\frac{R}{R_o}\right)-\frac{p_o}{\sigma_o}$$

$$\frac{\sigma_{YY}{}^{\rm V}}{\sigma_o}=-\sqrt{1-m^2}-\frac{1}{\sqrt{3}}\frac{mR_o}{T}\left[\left(1+\frac{R_1}{R_o}-\frac{R_2}{R_o}-2\frac{R_n}{R_o}-\frac{R_3}{R_o}+2\frac{R}{R_o}\right)+\left(\frac{Y}{R_o}\right)^2\frac{1}{R/R_o}-\frac{1}{4}\frac{1}{(R_o/T)^2}\frac{1}{R/R_o}\right]-\frac{p_o}{\sigma_o} \tag{56}$$

$$\frac{R_4}{R_o}\geq\frac{m}{4\sqrt{3}\,(1+\sqrt{1-m^2})\dfrac{R_o}{T}} \tag{57}$$

Zone VI.

$$\frac{\sigma_{RY}{}^{\rm VI}}{\sigma_o}=\frac{2}{\sqrt{3}}\frac{mR_o}{T}\left(\frac{Y}{R_o}\right)\left(\frac{\dfrac{R}{R_o}-\dfrac{R_i}{R_o}}{\dfrac{R_4}{R_o}-\dfrac{R_i}{R_o}}\right);\ \frac{\sigma_{R\Theta}{}^{\rm VI}}{\sigma_o}=\frac{\sigma_{\Theta Y}{}^{\rm VI}}{\sigma_o}=0$$

$$\frac{\sigma_{RR}{}^{\rm VI}}{\sigma_0}=-\left[\frac{1}{\sqrt{3}}\frac{mR_o}{T}\left(1+\frac{R_1}{R_o}-\frac{R_2}{R_o}-2\frac{R_n}{R_o}-\frac{R_3}{R_o}+2\frac{R_4}{R_o}\right)+\frac{p_o}{\sigma_o}\right]\left(\frac{\dfrac{R}{R_o}-\dfrac{R_i}{R_o}}{\dfrac{R_4}{R_o}-\dfrac{R_i}{R_o}}\right)+\frac{p_i}{\sigma_o}\left(\frac{\dfrac{R}{R_o}-\dfrac{R_4}{R_o}}{\dfrac{R_4}{R_o}-\dfrac{R_i}{R_o}}\right)$$

$$\frac{\sigma_{\Theta\Theta}{}^{\rm VI}}{\sigma_o}=-\left[\frac{1}{\sqrt{3}}\frac{mR_o}{T}\left(1+\frac{R_1}{R_o}-\frac{R_2}{R_o}-2\frac{R_n}{R_o}-\frac{R_3}{R_o}+2\frac{R_4}{R_o}\right)+\frac{p_o}{\sigma_o}\right]\left(\frac{2\dfrac{R}{R_o}-\dfrac{R_i}{R_o}}{\dfrac{R_4}{R_o}-\dfrac{R_i}{R_o}}\right)+\frac{2}{\sqrt{3}}\frac{mR_o}{T}\left[\frac{\dfrac{R}{R_o}\left(\dfrac{R}{R_o}-\dfrac{R_i}{R_o}\right)}{\dfrac{R_4}{R_o}-\dfrac{R_i}{R_o}}\right]+\frac{p_i}{\sigma_o}\left(\frac{2\dfrac{R}{R_o}-\dfrac{R_4}{R_o}}{\dfrac{R_4}{R_o}-\dfrac{R_i}{R_o}}\right) \tag{58}$$

$$\frac{\sigma_{YY}{}^{\rm VI}}{\sigma_o}=-\frac{1}{2}\left[\frac{1}{\sqrt{3}}\frac{mR_o}{T}\left(1+\frac{R_1}{R_o}-\frac{R_2}{R_o}-2\frac{R_n}{R_o}-\frac{R_3}{R_o}+2\frac{R_4}{R_o}\right)+\frac{p_o}{\sigma_o}\right]\left(\frac{3\dfrac{R}{R_o}-2\dfrac{R_i}{R_o}}{\dfrac{R_4}{R_o}-\dfrac{R_i}{R_o}}\right)$$

$$
-\frac{1}{\sqrt{3}}\frac{mR_o}{T}\left\langle\frac{\left(\dfrac{2\dfrac{R}{R_o}-\dfrac{R_i}{R_o}}{R/R_o}\right)\left[\left(\dfrac{Y}{R_o}\right)^2-\dfrac{1}{4(R_o/T)^2}\right]}{\left(\dfrac{R_4}{R_o}-\dfrac{R_i}{R_o}\right)}\right\rangle
$$

$$
+\frac{1}{\sqrt{3}}\frac{mR_o}{T}\left[\frac{\dfrac{R}{R_o}\left(\dfrac{R}{R_o}-\dfrac{R_i}{R_o}\right)}{\dfrac{R_4}{R_o}-\dfrac{R_i}{R_o}}\right]+\frac{1}{2}\frac{p_i}{\sigma_o}\left(\frac{3\dfrac{R}{R_o}-2\dfrac{R_4}{R_o}}{\dfrac{R_4}{R_o}-\dfrac{R_i}{R_o}}\right)
$$

$$
-\frac{1}{2}\sqrt{4\left[1-m^2\left(\frac{\dfrac{R}{R_o}-\dfrac{R_i}{R_o}}{\dfrac{R_4}{R_o}-\dfrac{R_i}{R_o}}\right)^2\right]-3\left\langle\left\{\frac{1}{\sqrt{3}}\frac{mR_o}{T}\left[\left(1+\frac{R_1}{R_o}-\frac{R_2}{R_o}-2\frac{R_n}{R_o}-\frac{R_3}{R_o}+2\frac{R_4}{R_o}\right)-2\left(\frac{R}{R_o}-\frac{R_i}{R_o}\right)\right]+\left(\frac{p_o}{\sigma_o}-\frac{p_i}{\sigma_o}\right)\right\}\left(\frac{R/R_o}{\dfrac{R_4}{R_o}-\dfrac{R_i}{R_o}}\right)\right\rangle^2}\;\Bigg)
$$

$$
\left\{\frac{1}{4\sqrt{3}}\frac{m}{R_o/T}\left[\frac{2\left(\dfrac{R_4}{R_o}\right)-\dfrac{R_i}{R_o}}{\left(\dfrac{R_4}{R_o}\right)\left(\dfrac{R_4}{R_o}-\dfrac{R_i}{R_o}\right)}\right]\right\}^2\leq +m^2+\frac{1}{4\sqrt{3}}\frac{m}{R_o/T}\left[\frac{2\left(\dfrac{R_4}{R_o}\right)-\dfrac{R_i}{R_o}}{\left(\dfrac{R_4}{R_o}\right)\left(\dfrac{R_4}{R_o}-\dfrac{R_i}{R_o}\right)}\right].
$$

$$
\times\sqrt{4(1-m^2)-3\left\langle\left\{\frac{1}{\sqrt{3}}\frac{mR_o}{T}\left(1+\frac{R_1}{R_o}-\frac{R_2}{R_o}-\frac{2R_n}{R_o}-\frac{R_3}{R_o}+\frac{2R_i}{R_o}\right)+\left(\frac{p_o}{\sigma_o}-\frac{p_i}{\sigma_o}\right)\right\}\left(\frac{R_4/R_o}{\dfrac{R_4}{R_o}-\dfrac{R_i}{R_o}}\right)\right\rangle^2} \qquad (59)
$$

$$
\frac{1}{4\sqrt{3}}\frac{m}{R_o/T}\left[\frac{1}{\dfrac{R_4}{R_o}-\dfrac{R_i}{R_o}}\right]\leqq\sqrt{4-3\left\langle\left[\frac{1}{\sqrt{3}}\frac{mR_o}{T}\left(1+\frac{R_1}{R_o}-\frac{R_2}{R_o}-2\frac{R_n}{R_o}-\frac{R_3}{R_o}+2\frac{R_4}{R_o}\right)+\left(\frac{p_o}{\sigma_o}-\frac{p_i}{\sigma_o}\right)\right]\left[\frac{R_i/R_o}{\dfrac{R_4}{R_o}-\dfrac{R_i}{R_o}}\right]\right\rangle^2} \qquad (60)
$$